Sound Source Identification of Vehicle Noise Based on a Microphone Array With a Modified Multiple Signal Classification Algorithm

Botong Wang

Department of Electrical Engineering and Information Technology, Technical University Darmstadt, Darmstadt, 64289, Germany.

Hui Guo and Canfeng Chen

School of Mechanical and Automotive Engineering, Shanghai University of Engineering Science, Shanghai, China.
E-mail: hgsues@163.com

(Received 31 January 2024; accepted 25 July 2024)

In this paper, a modified multiple signal classification (MUSIC) algorithm tailored for sound source identification (SSI) of vehicle noise is introduced and experimentally validated. A uniform planar microphone array (UPMA) is formulated for mathematical modeling, with its SSI-oriented parameters selected based on the primary frequency spectrum of vehicle noise. Simulations are conducted to compare the SSI accuracy of two conventional spatial spectra estimation (SSE) algorithms: the Capon algorithm and the MUSIC algorithm. The results demonstrate that the MUSIC algorithm, which relies on the eigenvalues of a covariance matrix to estimate signal direction, exhibits superior SSI resolution under low signal-to-noise ratio (SNR) conditions. However, it faces challenges in distinguishing between coherent or closely spaced signals. To address this, a modified MUSIC algorithm is proposed by reconstructing the covariance matrix of received signals and the SSE function. Simulation outcomes indicate that the modified MUSIC significantly outperforms the conventional version, owing to its enhanced SSI resolution. The accuracy of the SSI system, incorporating the UPMA and the modified MUSIC, is verified using a low-frequency volume source. Ultimately, the devised SSI system is successfully deployed to identify noise sources in a vehicle at different operational conditions, further validating the efficacy of the modified MUSIC. The UPMA and the modified MUSIC presented in this study have direct applicability in vehicle noise source identification and may be extended to other sound-related engineering fields for SSI purposes.

1. INTRODUCTION

Sound source identification (SSI) techniques, which may provide the energy distribution of a sound in a spatial domain, have been given more attention in vehicle noise control. The vehicle noise generated by the vibrations of structural parts, such as engine, powertrain, tire and exhaust system, etc., may lead to early fatigue damage of some parts, thus reducing the service life of the vehicle. Accurately determining the spatial locations of noise sources is helpful for analyzing the mechanism of noise and vibration, and can provide a basis for structural improvement and vibro-acoustic control of the vehicle. The SSI is one of the techniques used for signal source localization, which have been used in the fields of communications, radar, sonar, seismology and radio astronomy.[1] The commonly used SSI technologies are mainly involved in the aspects of microphone array design, source recognition algorithm and visualization.[2,3]

A microphone array consists of multiple microphones arranged by a certain rule. Due to the different spatial position of each array element and the amplitude and phase differences of the channels, the spatial location information of a sound source can be obtained by signal processing. Early microphone array technology was mainly used in the noise source recognition of large-scale products. Billingsley[4] and King[5] measured the sound field distributions of an aircraft engine and a high-speed train, respectively, by using linear microphone arrays. Fischer[6] established a model of an arc microphone array for identifying engine noise sources. Based on the theory of a one-dimensional (1D) linear array, a two-dimensional (2D) array was developed. Brooks[7] studied the airflow noise source of a helicopter using a 12-channel planar microphone array model. Piet8 and Michel[9,10] measured the noise sources on the surface and in the landing process of an aircraft by using a 39-channel cross-shaped microphone array and a 111-channel large-size planar array, respectively. Qiao[11] designed the regular and randomly optimized microphone arrays for source localization of aircraft landing and flap noises. To reduce the array size and improve its resolution, some parameter optimization techniques were introduced into the microphone array design. Mandal[12] used the particle swarm algorithm to optimize the line array and the planar array, in which the side-lobes were significantly reduced, but the resolution of the arrays is not high. An L-shape array was designed and optimized by using the genetic algorithm,[13] which effectively suppressed the grating lobes and side-lobes of the two-dimensional sparse arrays. To solve the problems of the two-dimensional arrays, such as incomplete acquisition of sound field information and poor imaging quality of sound source

identification, a three-layered three-dimensional (3D) microphone array was presented.[14] The experimental results showed that the designed array was superior to other two-dimensional arrays in both the sound source directivity and the side-lobe suppression. Then a new technique for automatically generating the 3D scanning surface for acoustic imaging using microphone arrays is proposed and more accurate results could be obtained.[15] This has advantages such as inexpensive and short scan time, which is tested using beamforming algorithms for a spherical array and an Underbrink multi-arm spiral array. A fast-beamforming method to localize an acoustic emission source in a thin-walled structure with unknown wave speed is proposed, which can more accurately localize the damage source than traditional delay-and-sum beamforming.[16] Comparatively, the 1D array can be easily designed, but it cannot provide the complete spatial information of a sound source. The 3D array may realize the spatial localization of a sound source, but its complex structure led to a high cost. Thus, a 2D microphone array with moderate performance and cost is adopted for vehicle noise source identification.

Early SSI approaches are subjective estimation, sound pressure measurement, separate operation, selective isolation, etc., which cannot obtain an accurate distribution of noise sources. Therefore, some techniques based on signal processing methods, such as spectral analysis, coherence function, surface intensity, near-field acoustical holography (NAH), beamforming, spatial spectrum estimation (SSE), etc., have been proposed in the past decades. Maynard17 first proposed the concept of NAH. Veronesi[18] extended the NAH to the cylindrical and spherical coordinates and successfully realized the holographic surface reconstruction of a non-planar sound source in discrete coordinates. To improve the NAH accuracy in equivalent sound source identification, Hald[19] proposed a statistically optimized NAH (SONAH) method, in which the sound field was reconstructed by using plane wave, evanescent wave and superposition coefficients. Considering the high requirement of array aperture for large-scale sound sources in the NAH, an extrapolation method based on data iteration in real and wavenumber spaces[20] and a patch NAH method based on fast Fourier transform[21] were successively proposed, which extend the NAH towards a quantitative technique in vibration and/or noise measurements for actual large-scale structures. For SSI of a vehicle noise, Yang[22] established the geometric relationship between the position and the time of a moving vehicle in a sound field, and obtained the visualization results of the noise source identification of a running vehicle. Although the NAH technology can obtain high-resolution SSI results, the signal acquisition must satisfy the near-field sound source condition and cannot be directly applied in many fields in engineering. The beamforming techniques based on delay-sum of multi-channel data can compensate for this deficiency.[23,24] To improve the resolution of the acoustic image, some methods, such as the cross-spectral delay-sum (CPDS), the deconvolution approach for mapping of acoustic sources (DAMAS) and the CLEAN based on spatial source coherence (CLEAN-SC), etc., have been introduced into SSI. Based on the binocular stereovision method, Yardibi[25–27] systematically compared the CPDS, DAMAS and CLEAN-SC algorithms, and the results suggest that the resolutions of the DAMAS and CLEAN-SC are higher than that of the CPDS. The DAMAS method has been successfully applied in noise source recognition of rotating machinery.[28]

Due to the Rayleigh limit, the acoustic images from the above beamforming methods have some problems, such as low resolution, pseudo source and high side-lobe, etc. To break through the Rayleigh limit, the SSE-based beamforming algorithms that use a spatial array to parameterize sound signals in a space have been developed. An early SSE-based algorithm proposed by Bartelett[29] cannot recognize the sound sources with a distance less than beam width. Capon[30] proposed an improved maximum likelihood estimation algorithm that can identify the sound sources with Gaussian distributions, however, needs to solve inverse autocorrelation matrix of signals and requires a large amount of computation. To reduce computational complexity, Schmidt[31] proposed the multiple signal classification (MUSIC) algorithm with higher resolution, in which the eigenvalues of the received signals are firstly decomposed, and then the orthogonality of noise subspace and signal subspace are utilized for sound source localization. Subsequently, an estimation of signal parameters via rotational invariance technique (ESPRIT)[32] was presented by establishing a solvable function based on the array characteristics and further searching the spectral peak on the function to estimate signal source direction. Considering the ESPRIT, furthermore, the high-resolution methods, so-called the CLEAN-SC with compressed grids (CLEAN-SC-CG)[33] and CLEAN with cross spectral matrix function (CLEAN-CSM)[34] were proposed based on the functional beamforming (FBF) and CLEAN. More recently, the Hilbert curve was introduced into the CLEAN-CSM, and a fast deconvolution method was developed,[35] which achieved a higher computation efficiency and a better dynamic range in the multi-sound sources localization. Currently, the most commonly used SSE algorithms are the MUSIC algorithm and its improved versions, such as the root-seeking MUSIC and the dimension reduction MUSIC algorithms[36–38] which are mainly applied in the fields of radar and sonar, but are rarely used for SSI of vehicle noise. Therefore, due to the characteristics of vehicle noise, it is still necessary to develop novel SSI approaches to for noise source identification in vehicle engineering.

Based on the above discussions, it can be found that the SSE-based algorithm can provide high-resolution SSI results by using a relatively small number of array microphones, and can overcome the shortcomings of the limitations of microphone number and measurement distance of the acoustic holography technique and low resolution of the traditional beamforming algorithm. The MUSIC algorithm suffers from a drawback: when multiple sources are coherent or close to each other, the covariance matrix of the array signals becomes rank-deficient, resulting in the MUSIC unable to distinguish them. The sources investigated in this study is an engine, which emit operational noise propagating through both air and solid mediums, resulting in multiple coherent sources within the engine compartment. By constructing a full-rank covariance matrix and introducing a new noise subspace, the modified MUSIC can identify the aforementioned coherent sources and closely spaced sources. Based on a self-designed microphone array, the noise source identification of the proposed method is ex-

perimentally verified, and the influences of array parameters on its output performance are investigated as well.

2. MICROPHONE ARRAY MODELING AND SETTING

2.1. Modeling For A Uniform Planar Array

This paper designs a uniform planar microphone array, as shown in Fig. 1. The uniform planar array with $M \times N$ elements in the $x-y$ plane was placed in the far field of the sound sources. The spacing among the elements was d. There were K sound sources in the space, and the sound signals satisfied the narrowband signal principle, which means the changes in sound waves were very small when passing through the array plane. θ_k and Φ_k represent the azimuth and pitch angles of the k th sound source with respect to the array plane, $k = 1, 2, 3, \cdots, K$. Thus, the wave path difference β between the ith array element and a reference element in the space may be expressed as:

$$\beta = 2\pi(x_i \cos\phi \sin\theta + y_i \sin\phi \cos\theta = z_i \cos\phi)/\lambda; \quad (1)$$

where, λ was the wavelength of a sound signal, (x_i, y_i, z_i) was the coordinate of the ith array element. For a planar array on the $x-y$ plane, $z_i = 0$. According to the theory of one-dimensional linear arrays, in the orientational matrix A_x with N array elements on the x-axis, the directional vector $a(\theta_k)$ of the kth sound source can be calculated by Eq. (2) (see top of the next page). The uniform array can be regarded as a combination of M rows and each row was a linear array with N elements. The directional matrix of the mth row in the array was in fact a phase offset of the first row along the y-axis. Therefore, the directional vector of the kth sound source on the y-axis can be defined as:

$$a_y(\theta_k) = \left[1 e^{=j2\pi \frac{d}{\lambda} \sin\theta_k \cos\phi_k} \cdots e^{=j2\pi(M-1)\frac{d}{\lambda} \sin\theta_k \cos\phi_k}\right]^T. \quad (3)$$

In case of the K sound sources, the orientational matrix in the y-axis direction A_y was:

$$A_y = [a_y(\theta_1) a_y(\theta_2) \cdots a_y(\theta_k)]. \quad (4)$$

Then, the orientational matrix of each row can be calculated by ${}_A x$ and A_y, i.e.,

$$\begin{cases} A_1 = A_x D_1(A_y) \\ A_2 = A_x D_2(A_y) \\ \vdots A_M = A_x D_M(A_y) \end{cases}; \quad (5)$$

where, $D_m(\dot{})$ was the diagonal matrix of the mth row. Thus, an orientational matrix $A_{M\times N}(\theta_k, \Phi_k)$ of the uniform planar microphone array can be rewritten in a form of matrix as in Eq. (6) (see top of the next page).

2.2. Parameter Selections For Planar Array

To design the uniform planar microphone array in Fig. 1, firstly, a minimum spacing d among the elements needed to be determined. To avoid a large level of side-lobes in sound source identification, the array design must satisfy the Nyquist sampling theorem, i.e., the sampling frequency should be two times greater than the frequency of interest of a signal. This relationship may be mathematically expressed by the spacing of array elements and the wavelength of sound waves:

$$d \le \frac{\lambda_{\min}}{2}. \quad (7)$$

In term of the array resolution that represents the identification ability of two adjacent sound sources, for a beam S on a reconstructed surface with a distance z from the sound source, the resolution of pitch angle θ can be calculated as:

$$R(\theta) = \frac{zR_s}{S\cos^3\theta}; \quad (8)$$

where, R_s was the width of the main lobe, $R_s = 0.866\ \lambda/D$, D denotes the array aperture, λ was the wavelength of the sound, z was the measurement distance, and θ was the angle between the incident direction of the sound wave and the normal line of the array plane. The relationship between the array resolution $R(\theta) \sim 1/\cos^3\theta$ and the incident direction angle θ of the sound was shown in Fig. 2. As can be seen that, the array resolution reduces with the angle θ increasing, and reduces rapidly when $\theta > 30°$. Therefore, in actual noise source identification, the angle between the normal line of the array plane and the incident direction of the sound wave should be set within $30°$ in order to ensure imaging resolution.

To investigate the influences of the array dimension and the element spacing on the acoustic pattern of the array, three sets of parameters of the uniform array model: (a) $M \times N = 2 \times 2, d = 0.5\lambda$, (b) $M \times N = 4 \times 4, d = 0.5\lambda$, and (c) $M \times N = 4 \times 4, d = 1.2\lambda$, were selected for acoustic pattern simulations in this study. The signal to noise ratio (SNR) was set to 30 dB, the number of snapshots is 500, and the sampling rate was 1024 Hz. The simulated output acoustic patterns are shown in Fig. 3.

Comparing the simulated results in Fig. 3 (a) and Fig. 3 (b), the array resolution improves with increasing of the element number. The results shown in Fig. 3 (a) and Fig. 3 (c) indicate that the element spacing follows the principle of minimum spacing principle. When the element spacing is greater than 0.5λ, a serious side-lobe phenomenon occurred, which affects the array pointing performance. Therefore, the uniform planar array was designed as a dimension of 4×4. For the stationary vehicle noise, the frequency range is mainly below 200 Hz. According to the principle of minimum spacing, the element spacing is determined as $d = 1/\lambda_{\min} = 15$ cm.

3. COMPARISON OF SSE ALGORITHMS FOR SOUND SOURCE IDENTIFICATION

The basic and typical SSE-based algorithms are the Capon and MUSIC algorithms. The MUSIC constructs a covariance matrix of signal vectors and maps them into the signal and noise subspaces according to the matrix eigenvalues. It utilizes the orthogonal characteristics of the subspaces to define a SSE function, and identifies the sound source by searching

$$A_X = [a(\theta_1)a(\theta_2)\cdots a(\theta_k)] = \begin{bmatrix} 1 & 1 & \cdots & 1 \\ e^{=j2\pi\frac{d}{\lambda}\sin\theta_1} & e^{=j2\pi\frac{d}{\lambda}\sin\theta_2} & \cdots & e^{=j2\pi\frac{d}{\lambda}\sin\theta_k} \\ & \cdots & \ddots & \vdots \\ e^{=j2\pi(M-1)\frac{d}{\lambda}\sin\theta_1} & e^{=j2\pi(M-1)\frac{d}{\lambda}\sin\theta_2} & \cdots & e^{=j2\pi(M-1)\frac{d}{\lambda}\sin\theta_k} \end{bmatrix}. \quad (2)$$

$$A_{M\times N}(\theta_1, \Phi_k) = \begin{bmatrix} 1 & e^{-j\frac{2\pi d}{\lambda}\sin\theta_2\cos\Phi_2} & \cdots & e^{-j\frac{2\pi d}{\lambda}(N-1)\sin\theta_k\cos\Phi_k} \\ e^{-j\frac{2\pi d}{\lambda}\sin\theta_1\cos\Phi_1} & e^{-j\frac{2\pi d}{\lambda}\sin^2\theta_2\cos\Phi_2\sin\Phi_2} & & e^{-j\frac{2\pi d}{\lambda}(N-1)\sin^2\theta_k\cos\Phi_k\sin\Phi_k} \\ \vdots & & \ddots & \vdots \\ e^{-j\frac{2\pi d}{\lambda}(M-1)\sin\theta_2\cos\Phi_2} & e^{-j\frac{2\pi d}{\lambda}(M-1)\sin^2\theta_2\cos\Phi_2\sin\Phi_2} & \cdots & e^{-j\frac{2\pi d}{\lambda}(N-1)(M-1)\sin^2\theta_k\cos\Phi_k\sin\Phi_k} \end{bmatrix}. \quad (6)$$

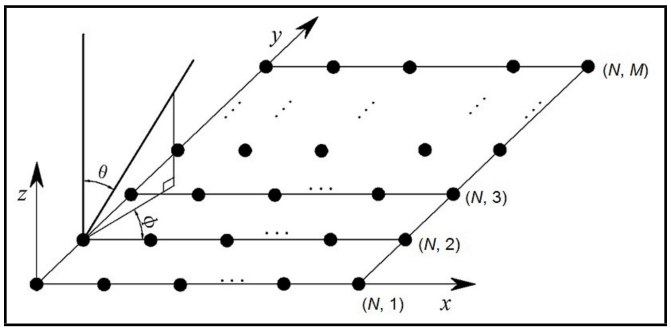

Figure 1. A model of uniform planar microphone array.

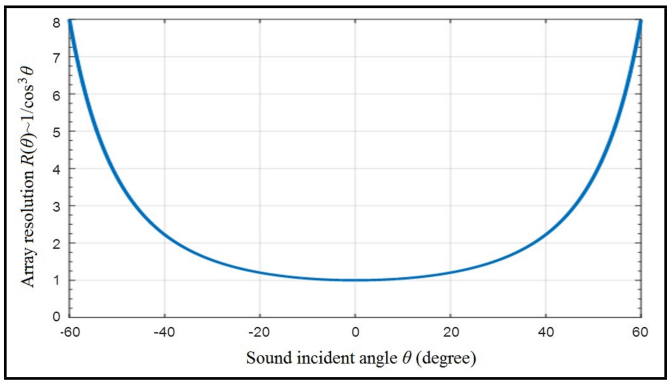

Figure 2. The relationship between the array resolution and the incident direction of a sound.

for spatial spectral peaks. The main sound source of a stationary vehicle is engine noise, which forms a continuous sound source surface on the vehicle body through air and/or solid propagations. To accurately obtain the sound source surface of the vehicle, this paper proposes a modified MUSIC algorithm. The results are compared to those of the Capon and MUSIC algorithms to demonstrate its superiority.

3.1. Modified MUSIC Algorithm

Assuming that, (a) the uniform planar array satisfies the minimum spacing condition in Eq. (7), (b) the sounds emitted by the sound sources are mutually independent narrowband signals, (c) the noises in received signals were uncorrelated Gaussian white noise with the same variance, and (d) the number of sound sources was less than the number of the array

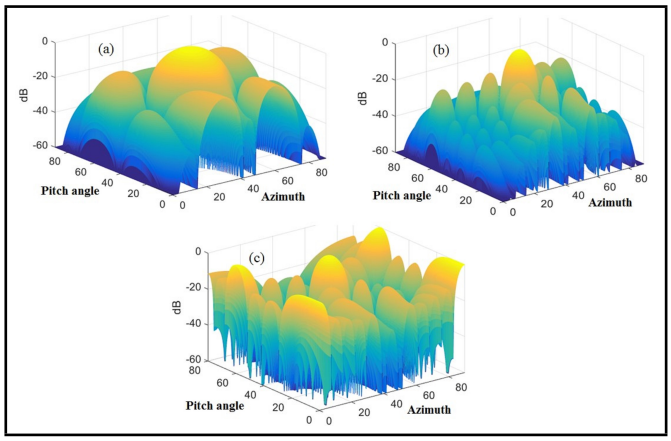

Figure 3. The output acoustic patterns of the designed uniform planar arrays: (a) $M \times N = 2 \times 2, d = 0.5\lambda$, (b) $M \times N = 4 \times 4, d = 0.5\lambda$, and (c) $M \times N = 4 \times 4, d = 1.2\lambda$

elements, the received sound signals can be described as,

$$X(t) = AS + N; \quad (9)$$

where, A was the directional matrix of the array, S was the signal source matrix and N was the received noise matrix. The covariance matrix R of the received signal may be calculated by,

$$R = E[X(t)X^H(t)] = APA^H + \sigma^2 I; \quad (10)$$

where, P was the covariance matrix of the spatial signals, and I was the unit matrix. H denotes the conjugate transpose of a matrix. Due to the independence of signal sources, P was a diagonal matrix, where the diagonal elements were powers of the signal. Because the number of sound sources was less than the number of array elements, R was full rank and can be decomposed into eigenvalues. However, the MUSIC algorithm also has its shortcomings. When there were two coherent signals or two signals that were very close to each other, the traditional MUSIC algorithm cannot distinguish them. It was necessary to restore the signal covariance matrix to a full-rank matrix. So, the MUSIC was modified following the below steps:

(a) Reconstruction for the covariance matrix R_x of the received signal:

$$R_x = 1/2(R + I_v R^* I_v); \quad (11)$$

where, I_v was the inverse unit matrix, and R^* was the conjugate matrix of R. Given that the covariance matrix R was Hermitian, R^* was equal to the transpose of R.

(b) Eigenvalue decomposition and subspace definition of the matrix R_x

$$R_x = U_s \Sigma_s U_s^H + U_n \Sigma_n U_n^H; \tag{12}$$

where, U_s and U_n were the decomposed eigenvectors of the signal subspace and the noise subspace, respectively. Here, $U_n \Sigma_n U_n^H$ was defined as the first noise subspace RN_{x1} and expressed as:

$$RN_{x1} = U_n \Sigma_n U_n^H = U_{n1} \Sigma_{n1} U_{n1}^H. \tag{13}$$

Replacing the R_x with the RN_{x1} and performing eigenvalue decomposition. Similarly, another noise subspace was obtained, which is named the second noise subspace RN_{x2}:

$$RN_{x2} = U_{n2} \Sigma_{n2} U_{n2}^H. \tag{14}$$

In a coherent acoustic environment, some of the signal energy leaks into the noise space. The difference between RN_{x1} and RN_{x2} was that the residual signal energy contained in the first noise subspace was greater than that in the second noise subspace. The two noise subspaces were partially coherent.

(c) Sum of the results in the noise subspaces obtained in step (b)

$$\begin{cases} U_n = U_{n1} + U_n 2 \\ \Sigma_n = \Sigma_{n1} + \Sigma_{n2} \end{cases}. \tag{15}$$

Thus, a new noise subspace can be defined as $RN = U_n \Sigma_n U_n^H$, and thereby a result of $Rnn = U_n \Sigma_n^{-1} U_n^H$. This processing procedure is like spatial smoothing algorithms, where the noise subspaces obtained from two decompositions maintain partial coherence with the signal subspace.

The coefficient 1/2 in Eq. (11) and the summation operation in Eq. (15) ensure that the noise energy remains consistent.

(d) Construction of the SSE function by substituting the Rnn:

$$P_{MUSIC}(\theta) = \frac{1}{a^H(\theta) Rnn Rnn^H a(\theta)}. \tag{16}$$

3.2. Simulation Experiments And Discussions

The Capon, the traditional MUSIC and the modified MUSIC algorithms were simulated and compared in this study. Firstly, the simulation conditions were set as follows: The dimension of the uniform planar array is 44, and the element spacing is $d = 0.5\lambda_{\min}$. Two sound sources located at $[\theta_1, \Phi_1] = [30^\circ, 30^\circ]$, $[\theta_2, \Phi_2] = [100^\circ, 120^\circ]$ were assumed in the space. The distance between the two sound sources and the array plane was 2 m. The SNRs of the two sound sources were set to $SNR = [30, 10]$ dB. In the simulations, the number of snapshots was 500, and the sampling frequency was 1024 Hz. The simulated results of the Capon and the MUSIC algorithms are shown and compared in Fig. 4. On the surfaces of the left panels in Fig. 4 (a) and (b), there were two obvious spectral peaks at the positions $[30^\circ, 30^\circ]$ and $[100^\circ, 120^\circ]$, indicating that the Capon and the MUSIC can identify the orientations of the sound source in the space. Comparing the contour lines of the results identified by the two algorithms shown in the right panels in Fig. 4, the MUSIC algorithm has a more concentrated output energy at the second sound source position $[100^\circ, 120^\circ]$, although the $SNR = 10$ was lower than that used in the Capon. This indicates that MUSIC has higher resolution and more accurate that the Capon algorithm.

To verify the performance of modified MUSIC, firstly, the simulations of the traditional and modified MUSIC algorithms were performed based on a virtual 1D linear array. The conditions were set as follows: three sound sources at the positions of $\theta = [-20^\circ, 11^\circ, 14^\circ]$ were 2 m away from the array line, the spacing of the array elements was $d = 0.5\lambda_{\min}$, the number of array elements was $M = 8$, the SNR was 10 dB, the number of snapshots was 500 and the sampling frequency was 1024 Hz. The simulated results are shown in Fig. 5. The two algorithms can give an obvious peak at the position of $\theta = -20^\circ$. However, the traditional MUSIC only shows a broadband peak in the angle range of $[11^\circ 14^\circ]$ and cannot distinguish the sound sources with small distance. The modified MUISC algorithm can obtain definite energy peaks at the positions of $\theta = [-20^\circ, 11^\circ, 14^\circ]$, which implies that the modified version of MUISC algorithm has a higher resolution for signal source identification comparing with the traditional one. To examine the estimation errors, by changing the conditions $\theta = 50^\circ$ and $SNR = [-10, -8, -6, -4, -2, 0, 2, 4, 6, 8, 10]$, the direction of arrival (DOA) estimations of the MUSIC and the modified MUSIC are conducted. The root mean square (RMS) errors of the two algorithms for the same sound source are shown in Fig. 6. Comparison of the RMS errors shows that the estimated errors of the two algorithms decrease with increasing of the SNR. The estimated error of the modified MUSIC is obviously less than that of the traditional one at low SNRs, and the difference of RMS errors between the two algorithms gradually decreases with the increase of SNR. Thus, it can be concluded that the modified MUSIC algorithm has higher accuracy and stronger anti-noise ability in sound source recognition.

Furthermore, the simulations of the traditional and modified MUSICs are expanded to 2D space by assuming a uniform planar array for comparing their capability to identify two sound sources with a very small distance. The simulation conditions were as follows: the distance from sound source to array plane was 2 m, the planar array with a dimension of 4×4 had a uniformed spacing $d = 0.5\lambda_{\min}$ among the elements, The sound source positions were set to $[45^\circ, 45^\circ]$ and $[60^\circ, 80^\circ]$, i.e., the signal azimuths were 45° and 60°, and the pitch angles were 45° and 80°, the SNRs were set to 5, 15 and 20 dB, respectively, the number of snapshots was 500, and the sampling frequency was 1024 Hz. The 2D simulated SSI results with the SNR equals to 5 dB, 15 dB and 20 dB are shown in Figs. 7, 8 and 9, respectively. Comparing the simulated results in Figs. 8, 9 and 10, the conclusions can be drawn that, in case of identification for two very close sound sources, the traditional MUSIC algorithm only has one peak in the identification results, while the modified MUSIC algorithm yields two peaks that appear at the positions $[45^\circ, 45^\circ]$ and $[60^\circ, 80^\circ]$ (without "confusion" phenomenon), which are exactly consistent with the assumed sound source positions. Under the conditions of the same SNRs, the obtained spectral peaks from the modified MUSIC are obviously higher than those from the traditional one, which implies that the modified MUSIC has a higher SSI resolution. The obtained spatial spectral peaks of

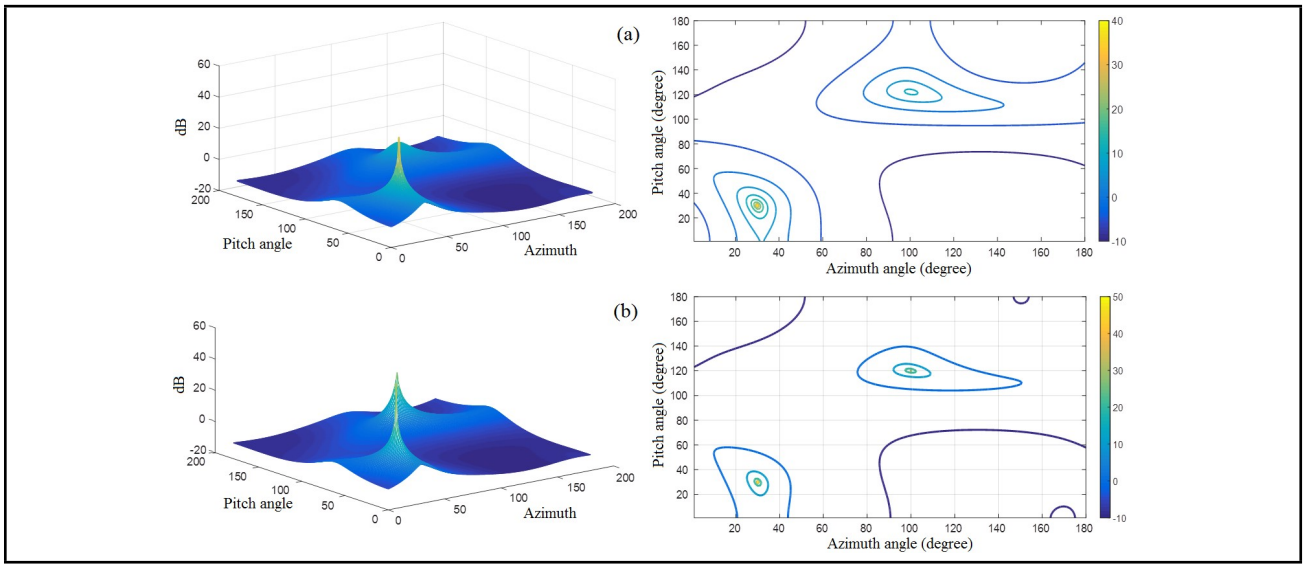

Figure 4. Comparison of the sound source identification results of (a) the Capon and (b) the MUSIC algorithms.

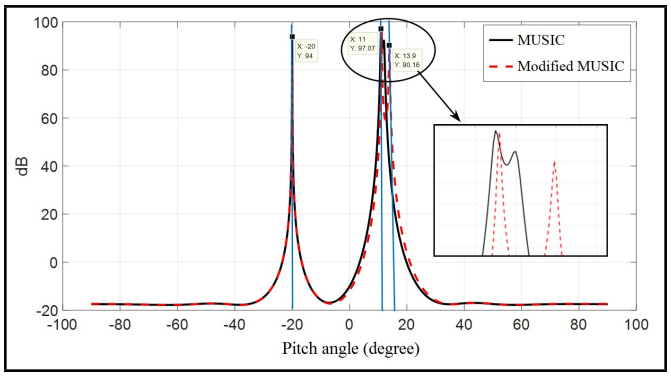

Figure 5. Comparison of the simulation results from the MUSIC and the modified MUSIC algorithms.

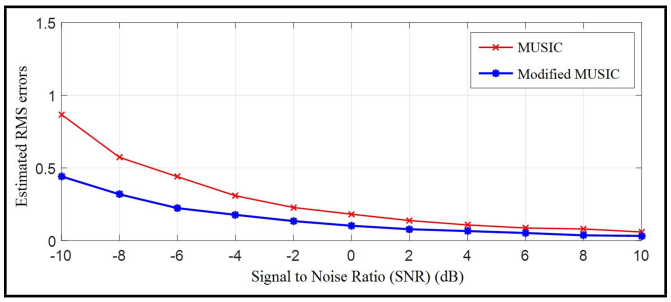

Figure 6. The estimated RMS errors obtained from the MUSIC and the modified MUSIC algorithms.

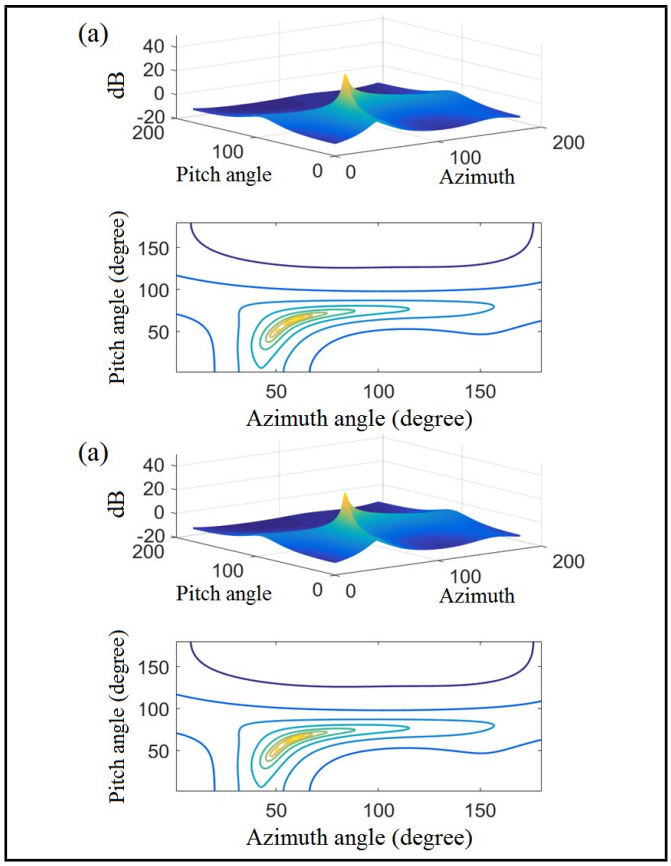

Figure 7. The simulated results from (a) the traditional MUSIC and (b) the modified MUSIC algorithms (SNR=5dB).

the traditional and modified MUSIC algorithms increase with increasing of SNR, which suggests that the SNR needs to be effectively controlled in application of the MUSICs in engineering.

From the above simulations and discussions, it can be concluded that the modified MUSIC presented in this paper can obtain exact results in sound source identifications. In terms of the resolution, RMS error and SSI accuracy, the modified MUSIC algorithm is superior to the Capon and the traditional MUSIC algorithms, and might be a promising approach for SSI of vehicle noise.

4. EXPERIMENTAL VERIFICATION OF MODIFIED MUSIC ALGORITHM

To prove the modified MUSIC algorithm in practical applications, furthermore, an experimental verification is conducted in this paper. The experimental setting[39] is shown in Fig. 10 and the corresponding equipment is listed in Tab. 1. A uniform planar array with a dimension of 4×4 (16 microphones) and the same microphone spacing of $d = 15$ cm was designed and made for sound source identification. The 4×4 uniform planar array and a 40-channel LMS-SCM data acquisition system

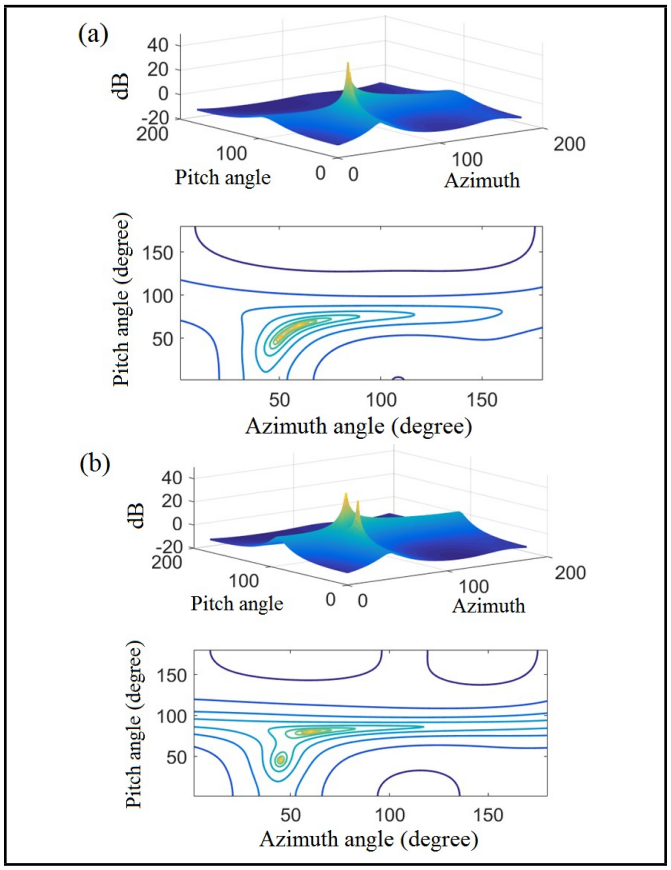

Figure 8. The simulated results from (a) the traditional MUSIC and (b) the modified MUSIC algorithms (SNR=10dB).

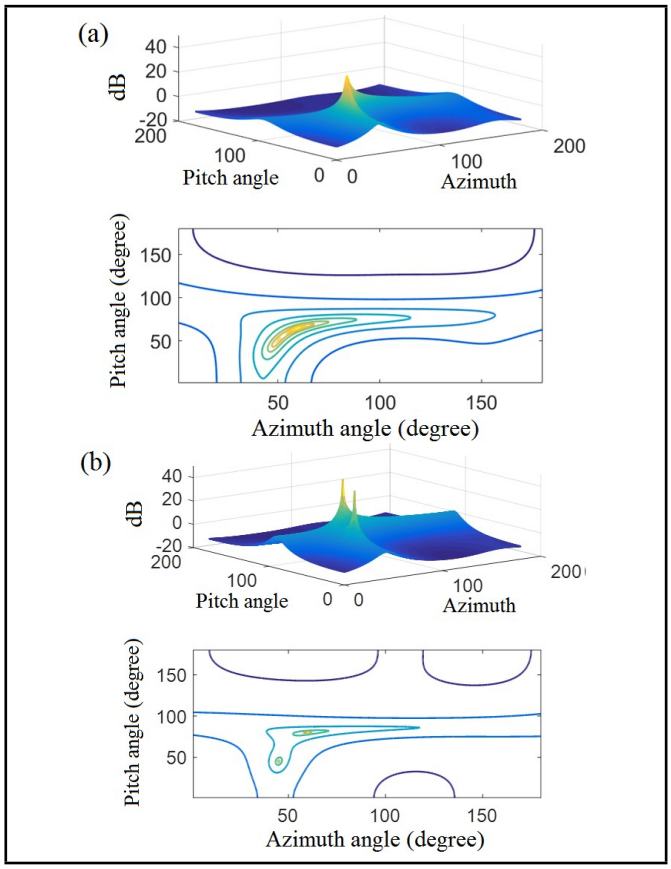

Figure 9. The simulated results from (a) the traditional MUSIC and (b) the modified MUSIC algorithms (SNR=15dB).

were used to collect the sound signals from a low-frequency volume sound source Q-LMF. The sounds in a low-frequency range similar to the engine noise of a vehicle were given by the volume sound source, and the excitation signals were provided by the LMS-SCM system. The square microphone array with a size of 45 cm $\times$ 45 cm was placed directly opposite the volume sound source, and the distance between the array plane and the sound source was 1.2 m to meet the requirement of a far-field configuration. Taking the microphone in the lower left corner of the array as a reference, considering the spatial position relationship of the volume sound source to the reference position, the centre coordinates of the sound source were calculated as $[18°, 16°]$. In accordance with the reconstruction surface rule, the volume sound source was placed in the reconstruction surface of the sound source. In experiments, the sampling rate was set to 1024 Hz according to the Nyquist sampling theorem. The data collection duration was set to 30 s. Three experiments were conducted by setting the sound signal frequencies as 100 Hz, 120 Hz and 150 Hz, respectively.

The data collected from the experiments 1, 2 and 3 were imported into the sound source identification program based on the modified MUSIC algorithm. The calculated SSI results are given in Fig. 11 and Tab. 2. The SSI results show that the modified MUSIC algorithm can successfully identify the angular position of the sound source relative to the microphone array.

From experiment results in Fig. 11 and Tab. 2, it can be found that, three experiments produce significant spectral peaks near the reference position of $[18°, 16°]$, indicating that the experiments can identify the position of the sound source.

Table 1. The experimental equipment selected for sound source identification.

Equipment name	Company	Type
Microphone	PCB	378B02
Microphone calibrator	B&K	4231
Data acquisition system	Siemens	LMS-SCM 05
Power amplifier	Siemens	Q-AMP
Volume sound source	Siemens	Q-LMF
Host computer	Dell	Inspiron 14R SE 7420

Table 2. Identified azimuth and pitch angles of the sound source.

Item	Azimuth angle (degree)	Pitch angle (degree)	SSI error (degree)
Actual position	18	16	–
Experiment 1	18	16	[0, 0]
Experiment 2	19	15	[1,-1]
Experiment 3	18	17	[0, 1]

Through the contours of the three experiments shown in the right panels of Fig. 11 and the SSI errors listed in Tab. 2, relative to the fixed position of the sound source at the angular coordinate $[18°, 16°]$, The azimuth angle errors of the three experimental results are $[0°, 1°, 0°]$, corresponding to the pitch angle errors of $[0°, 1°, 0°]$. The SSI errors are $\pm 1°$. Many studies have suggested that the error range of the azimuth and pitch angles is generally between $\pm 2°$ and $\pm 5°$ in the SSI engineering. The obtained SSI errors are acceptable, because they are within the allowable error range. These experimental results suggest that the modified MUSIC algorithm has good stability and accuracy, and is effectively in practical sound source identifications.

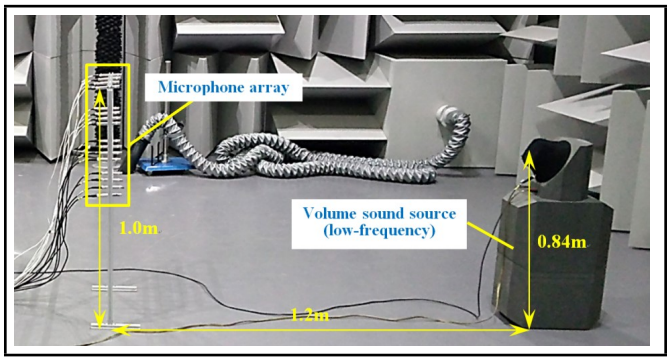

Figure 10. Arrangements of a sound source and the microphone array.

5. CONCLUSION

This paper proposes a modified MUSIC tailored for the identification of low-frequency vehicle noise sources. The approach integrates the uniform planar microphone array technique with a spatial spectra estimation (SSE) algorithm. Derived from the traditional MUSIC, the modified MUSIC equations are formulated through the reconstruction of the covariance matrix. Both simulations and experiments are conducted to validate the modified MUSIC's efficacy in sound source identification (SSI). Simulation results indicate that the modified MUSIC outperforms both Capon and the traditional MUSIC in terms of resolution, root mean square (RMS) error, and SSI accuracy. Subsequently, a self-designed microphone array is employed to verify the modified MUSIC's performance, demonstrating its high stability and accuracy in SSI applications. Finally, the modified MUSIC, alongside the self-designed microphone array, is applied to identify noise sources from a stationary vehicle in a semi-anechoic chamber. Observations reveal that as engine speed escalates, the primary noise source shifts position. The established SSI system, grounded in the modified MUSIC and the uniform planar microphone array, offers exceptional stability and accuracy, making it a viable solution for vehicle noise source identification.

ACKNOWLEDGEMENTS

This work was supported by the Project of National Natural Science Foundation of China (No. 52172371), and partly sponsored by the Program for Shanghai Academic Research Leader (No. 21XD1401100) and the Project of Technical Service Platform for Noise and Vibration Evaluation and Control of New Energy Vehicles (No. 18DZ2295900) at Science and Technology Commission of Shanghai Municipality, China.

REFERENCES

[1] A. Glowacz, Fault diagnosis of single-phase induction motor based on acoustic signals, *Mechanical Systems and Signal Processing*, **117**, 65-80, (2019). https://doi.org/10.1016/j.ymssp.2018.07.044

[2] M. Mršnik, J. Slavič, M. Boltežar, Vibration fatigue using modal decomposition, *Mechanical Systems and Signal Processing*, **98**, 548-556, (2018). https://doi.org/10.1016/j.ymssp.2017.03.052

[3] I. Thng, A. Cantoni, Y. Leung, Derivative constrained optimum broad-band antenna arrays, *IEEE Transactions on Signal Processing*, **41**(7), 2376-2388, (1993). https://doi.org/10.1109/78.224247

[4] J. Billingsley, R. Kinns, The acoustic telescope, *Journal of Sound and Vibration*, **48**(4), 485-510, (1976). https://doi.org/10.1016/0022-460X(76)90552-6

[5] W. King III, D. Bechert, On the sources of wayside noise generated by high-speed trains. *Journal of Sound and Vibration*, **66**(3), 311-332, (1979). https://doi.org/10.1016/0022-460X(79)90848-4

[6] M. Fisher, M. Harper-Bourne, S. Glegg, Jet engine noise source location: the polar correlation technique, *Journal of Sound and Vibration*, **51**(1), 23-54, (1977). https://doi.org/10.1016/S0022-460X(77)80111-9

[7] T. Brooks, M. Marcolini, D. Pope, A directional array approach for the measurement of rotor noise source distributions with controlled spatial resolution, *Journal of Sound and Vibration*, **112**(1), 192-197, (1987). https://doi.org/10.1016/S0022-460X(87)80105-0

[8] J. Piet, G. Elias, Airframe noise source localization using a microphone array, *The 3rd AIAA/CEAS Aeroacoustics Conference*, Atlanta, 91-466, (1997). https://doi.org/10.2514/6.1997-1643

[9] U. Michel, B. Barsikow, B. Haverich, M. Schüttpelz, Investigation of airframe and jet noise in high-speed flight with a microphone array, *The 3rd AIAA/CEAS Aeroacoustics Conference*, Atlanta, 97-1596, (1997). https://doi.org/10.2514/6.1997-1596

[10] U. Michel, J. Helbig, B. Barsikow, M. Hellmig, M. Schuettpelz, Flyover noise measurements on landing aircraft with a microphone array, *The 4th AIAA/CEAS Aeroacoustics Conference*, Toulouse, 98-2336, (1998). https://doi.org/10.2514/6.1998-2336

[11] W. Y. Qiao, U. Michel, Landing noise of aircraft based on the fly-over measurements with a planar microphone array, *Chinese Journal of Acoustics (English Edition)*, **21**(1), 9-22, (2002). link.cnki.net/doi/10.15949/j.cnki.0217-9776.2002.01.002

[12] D. Mandal, S. Das, S. Bhattacharjee, Linear antenna array synthesis using novel particle swarm optimization, *IEEE Symposium on Industrial Electronics & Applications*, Kolkata, 311-316, (2011). https://doi.org/10.1109/ISIEA.2010.5679450

[13] C. Feng, H. Ye, H. Hong, E. Wang and X. Zhu, A Hybrid Algorithm for Sparse Antenna Array Optimization of MIMO Radar, *2022 IEEE Radio and Wireless Symposium (RWS)*, Las Vegas, NV, USA, 115-117, (2022). https://doi.org/10.1109/RWS53089.2022.9719968

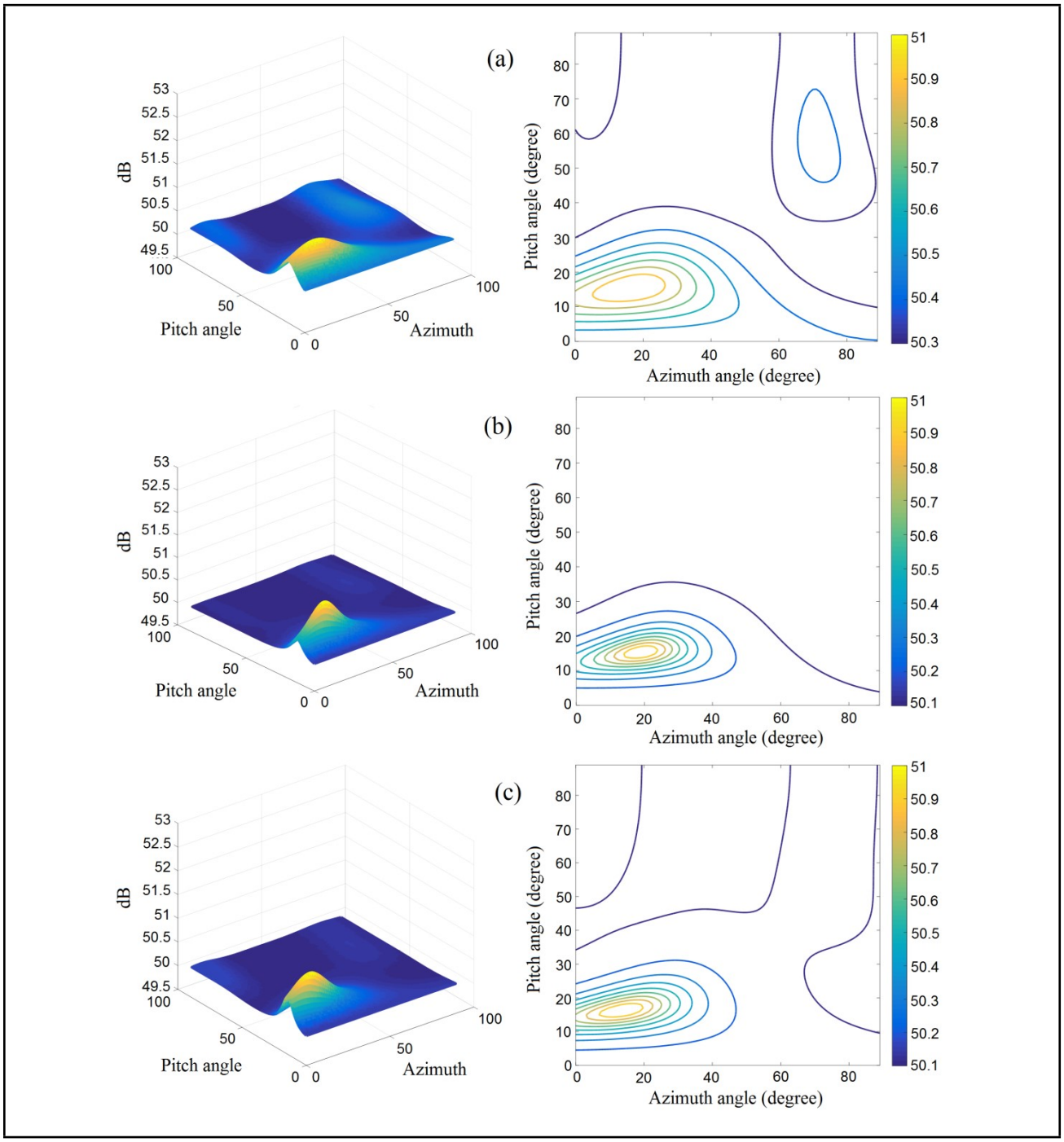

Figure 11. SSI results by using a volume sound source: (a) experiment 1, (b) experiment 2 and (c) experiment 3.

[14] Y. Zhang, C. Bi, L. Xu, X. Chen, Novel Method for Selection of Regularization Parameter in the Near-field Acoustic Holography, *Chinese Journal of Mechanical Engineering*, **24**(2), 285-292, (2011). https://doi.org/10.3901/cjme.2011.02.285

[15] M. Legg, S. Bradley, Automatic 3D scanning surface generation for microphone array acoustic imaging, *Applied Acoustics*, **76**, 230-237, (2014). https://doi.org/10.1016/j.apacoust.2013.08.008.

[16] J. Tai, T. He, Q. Pan, D. Zhang, X. Wang, A fast beamforming method to localize an acoustic emission source under unknown wave speed, *Materials*, **12**, 735, (2019). https://doi.org/10.3390/ma12050735

[17] J. Maynard, E. Williams, Y. Lee Nearfield acoustic holography: I. Theory of generalized holography and the development of NAH, *Journal of the Acoustical Society of America*, **78**(4), 1395-1413, (1985). https://doi.org/10.1121/1.392911

[18] W. A. Veronesi, J. Maynard, Nearfield acoustic holography (NAH): II. Holographic reconstruction algorithms and computer implementation, *Journal of the Acoustical Society of America*, **81**(5), 1307-1322, (1987). https://doi.org/10.1121/1.394536

[19] J. Hald, Reduction of spatial windowing effects in acoustical holography, *Proceedings of Inter-Noise 94*, Yokohama, Japan, 1887-1890, (1994). ince.publisher.ingentaconnect.com/content/ince/incecp/1994/00001994/00000003/art00097

[20] K. Saijyou, S. Yoshikawa, Reduction methods of the reconstruction error for large-scale implementation of near-field acoustical holography, *Journal of the Acoustical Society of America*, **110**(4), 2007-2023, (2001). https://doi.org/10.1121/1.1405417

[21] J. Hald, F. Nielsen, C. Blaabjerg, Patch NAH for Noise Source Mapping in Cabin Environments, *SAE Technical Paper*, 2005-01-2538, (2005). https://doi.org/10.4271/2005-01-2538

[22] D. Yang, S. Zheng, B. Li, K. Li, X. Lian, Video visualization for moving sound sources based on binoculars stereo and acoustic holography Source, *Chinese Journal of Acoustics*, **35**(2), 203-213, (2011). link.cnki.net/doi/10.15949/j.cnki.0217-9776.2011.02.010

[23] Y. Zhang, F. Jacobsen, C. Bi, X. Chen. Near field acoustic holography based on the equivalent source method and pressure-velocity transducers. *Journal of the Acoustical Society of America*, **126**(3), 1257-1263, (2009). https://doi.org/10.1121/1.3179665

[24] S. Gade, J. Hald, Noise source identification with increased spatial resolution used in automotive industry, *Journal of the Acoustical Society of America*, **131**(4), 3220-3220, (2012). https://doi.org/10.1121/1.4708008

[25] T. Yardibi, J. Li, P. Stoica, N. Zawodny, L. Cattafesta III, A covariance fitting approach for correlated acoustic source mapping, *Journal of the Acoustical Society of America*, **127**(5), 2920-2931, (2010). https://doi.org/10.1121/1.3365260

[26] T. Yardibi, J. Li, P. Stoica, L. Cattafesta III, Sparsity constrained deconvolution approaches for acoustic source mapping, *Journal of the Acoustical Society of America*, **123**(5), 2631-2642, (2008). https://doi.org/10.1121/1.2896754

[27] T. Yardibi, N. Zawodny, C. Bahr, F. Liu, L. Cattafesta III, N. Louis, J. Li, Comparison of microphone array processing techniques for aeroacoustic measurements, *International Journal of Aeroacoustics*, **9**(6), 733-761, (2010). https://doi.org/10.1260/1475-472x.9.6.733

[28] W. Pannert, C. Maier, Rotating beamforming-motion-compensation in the frequency domain and application of high-resolution beamforming algorithms. *Journal of Sound and Vibration*, **333**(7), 1899-1912, (2014). https://doi.org/10.1016/j.jsv.2013.11.031

[29] H. Krim, M. Viberg, Two decades of array signal processing research: the parametric approach, *IEEE Signal processing magazine*, **13**(4), 67-94, (1996). https://doi.org/10.1109/79.526899

[30] J. Capon, High-resolution frequency-wavenumber spectrum analysis. *Proceedings of the IEEE*, **57**(8), 1408-1418, (1969). https://doi.org/10.1109/proc.1969.7278

[31] R. Schmidt, Multiple emitter location and signal parameter estimation, *IEEE Transactions on Antennas and Propagation*, **34**(3), 276-280, (1986). https://doi.org/10.1109/tap.1986.1143830

[32] R. Roy, T. Kailath, ESPRIT-estimation of signal parameters via rotational invariance techniques. *IEEE Transactions on Acoustics, Speech, and Signal Processing*, **37**(7), 984-995, (1989). https://doi.org/10.1109/29.32276

[33] Y. Wang, C. Yang, Y. Wang, D. Hu, A fast deconvolution algorithm based on compressed focus grid points, *Journal of Vibration and Shock*, **41**(6), 250-255, (2022). link.cnki.net/doi/10.13465/j.cnki.jvs.2022.06.032

[34] Y. Wang, C. Yang, Y. Wang, D. Hu, R. Gu, Multi-source identification method based on cross-spectral matrix function, *Journal of Vibration, Measurement and Diagnosis*, **43**(2), 277-281, (2023). link.cnki.net/doi/10.16450/j.cnki.issn.1004-6801.2023.02.010

[35] C. Yang, Y. Wang, Y. Wang, H. Guo, D. Hu, A fast deconvolution method for multiple sound source localization based on Hilbert curve, *Digital Signal Processing*, **133**, 103872, (2023). https://doi.org/10.1016/j.dsp.2022.103872

[36] C. Qian, L. Huang, H. So. Improved unitary root-MUSIC for DOA estimation based on pseudo-noise resampling, *IEEE Signal Processing Letters*, **21**(2), 140-144, (2014). https://doi.org/10.1109/LSP.2013.2294676

[37] A. Hassanien, S. Vorobyov, Y. Yoon, J. Park, Root-MUSIC based source localization using transmit array interpolation in MIMO radar with arbitrary planar arrays, *The 5th International Workshop on Computational Advances in Multi-Sensor Adaptive Processing (CAMSAP)*, 396-399, (2013). https://doi.org/10.1109/camsap.2013.6714091

[38] W. Wang, X. Wang, X. Li, H. Song, DOA estimation for monostatic MIMO radar based on unitary root-MUSIC, *International Journal of Electronics*, **100**(11), 1499-1509, (2013). https://doi.org/10.1080/00207217.2012.751319

[39] ISO 5130-2019: Acoustics–Measurements of sound pressure level emitted by stationary road vehicles, (2019). https://doi.org/10.3403/30114830